Received 7 December 2019; revised 12 February 2020 and 15 March 2020; accepted 3 April 2020. Date of publication 8 April 2020; date of current version 29 April 2020. The review of this article was arranged by Editor T.-L. Ren.

Digital Object Identifier 10.1109/JEDS.2020.2986261

Thermal Field Analysis for New AlGaN/GaN HEMT With Partial Etched AlGaN Layer

BAOXING DUAN, LUOYUN YANG, HAO WU, AND YINTANG YANG

Key Laboratory of the Ministry of Education for Wide Band-Gap Semiconductor Materials and Devices, School of Microelectronics, Xidian University, Xi'an 710071, China

CORRESPONDING AUTHOR: B. DUAN (e-mail: bxduan@163.com)

This work was supported in part by the Science Foundation for Distinguished Young Scholars of Shaanxi Province under Grant 2018JC-017, and in part by the 111 Project under Grant B12026.

ABSTRACT In order to explore the distribution of the device temperature field, this paper takes the new AlGaN/GaN HEMT with partial etched AlGaN layer as the research object. First, the ISE TCAD software is used to simulate the temperature field of AlGaN/GaN HEMT in two dimensions. The simulation results show a decrease of the maximum temperature and average junction temperature in the device channel with shorter thickness of the etched AlGaN layer. As the etching length increases, the hot spot temperature near the gate edge decreases, and the new hot spot position gradually shifts to the drain, which results in a more uniform distribution in the channel. Then, Raman spectroscopy is used to measure the channel junction temperature of AlGaN/GaN HEMTs. The results indicate that when the power dissipation is 0.3W and the etching depth is 5, 10, 15nm, the average channel junction temperature of the new etched AlGaN/GaN HEMT is 9.7%, 17.4% and 30.3% lower than that of the ordinary AlGaN/GaN HEMT, respectively. And the highest temperature of the new AlGaN/GaN HEMT also decreases. We can see that etching the barrier layer of AlGaN/GaN HEMT can not only improve the breakdown voltage, but also effectively reduce the channel junction temperature, and establish the relationship between the high power and thermal stability of the AlGaN/GaN HEMTs.

INDEX TERMS Temperature field, AlGaN/GaN HEMT, raman spectroscopy, thermal stability.

I. INTRODUCTION

The third-generation wide band gap semiconductor material GaN has been widely used in microwave power devices due to its unique advantages such as wide bandgap, critical breakdown electric field intensity, high electron mobility and high electron saturation rate. AlGaN/GaN HEMT has become a research hotspot because of the high mobility of two-dimensional electron gas on the interface of AlGaN/GaN heterojunction [1]–[3]. However, when AlGaN/GaN HEMT is working under high voltage and high current for a long time, the temperature in the device will also increase. This will bring many adverse effects, such as increasing gate leakage current, reducing transconductance and leakage saturation current. This phenomenon is called the self-heating effect [4], [5]. The existence of self-heating effect will not only affect the device performance, but also reduce the reliability. In severe cases, it will even cause irreversible degradation. Therefore, it is important for us to study the temperature distribution in the AlGaN/GaN HEMTs.

At present, researchers have analyzed the temperature field of devices from different angles. Firstly, the numerical analysis model of junction temperature distribution is studied. The appropriate analytical model can help predict the actual temperature distribution. In 2007, Heller and Crespo combined the electrothermal model of the HEMT with the three-dimensional coupled thermal model of the substrate, and got the distribution of the junction temperature with the bias condition of the device, the substrate condition and the grid index parameters [6]. In 2017, Aouf *et al.* studied the influence of self-heating on the performance of GaN devices. The analytical model of drain current, power dissipation and lattice temperature were proposed [7]. Secondly, the temperature field of the device is simulated by software. The key problem is how to add the appropriate physical model.

In addition, Bertoluzza *et al.* first used the three-dimensional finite element analysis method to simulate the temperature distribution of the AlGaN/GaN HEMT in 2009 [8]. Finally, the actual temperature distribution of the device has been measured and studied. At present, the main methods used to measure the temperature of AlGaN/GaN HEMTs are electrical method, photoluminescence technology, infrared thermal imaging technology, and Raman spectroscopy [9]–[11]. Since these methods have different characteristics based on different physical principles, we need to make a choice according to the actual situation of the equipment to be tested. As well as the requirement of measurement accuracy, the Raman spectroscopy method is adopted.

In this paper, aimed at the AlGaN/GaN HEMT with partial etched AlGaN barrier layer proposed by Duan Baoxing [12], we study the temperature distribution under working condition from two aspects of software simulation and practical testing, and the effect of etched AlGaN barrier layer on device temperature distribution is explored. EAL-HEMT is used as an abbreviation for the novel AlGaN/GaN HEMT. First, we use ISE TCAD software to simulate the two-dimensional temperature field of the device, and the variation of channel junction temperature with device parameters under the same bias conditions is observed. By observing the temperature distribution of the device along the substrate, we find that the heat is mainly concentrated between the AlGaN/GaN heterojunction and the surface. Due to the thinner thickness of the AlGaN barrier layer, we mainly pay attention to the temperature distribution in AlGaN/GaN heterojunction interface. Then, in order to obtain more accurate measurement results, this paper uses Raman spectroscopy to measure the actual junction temperature distribution. The gate bias voltage of V_{GS} is 0V, and the drain bias voltage V_{DS} is changed to gain different power dissipation.

II. DEVICE STRUCTURE AND DESCRIPTION

The structure of the device studied in this paper is shown in Fig. 1 (a). The Al component of the AlGaN barrier layer is 0.25. The simulation parameters of the new AlGaN/GaN HEMT with partial etched AlGaN layer are shown in Table 1. In this paper, ISE TCAD software is used to simulate the temperature field distribution, and appropriate thermal field physical models are added to the simulation. The main physical models include the high-field mobility saturation model, the composite model of temperature-dependent carrier generation, the thermodynamic model and the thermo-electronic model.

Fig. 1 (b) is microscopic photos of fabricated EAL-HEMT. The fabricated EAL-HEMT used in experiment is AlGaN/GaN heterojunction structure on sapphire substrate. GaN buffer layer is grown along sapphire substrate (0001) direction by MOCVD. The thickness of GaN layer is 1.8μm, of which 1.5μm is doped by P-type. The purpose of P-type doping is to obtain GaN buffer layer and reduce the intrinsic carrier concentration in GaN. The thickness of AlGaN barrier layer is 20nm and the Al component is 32%.

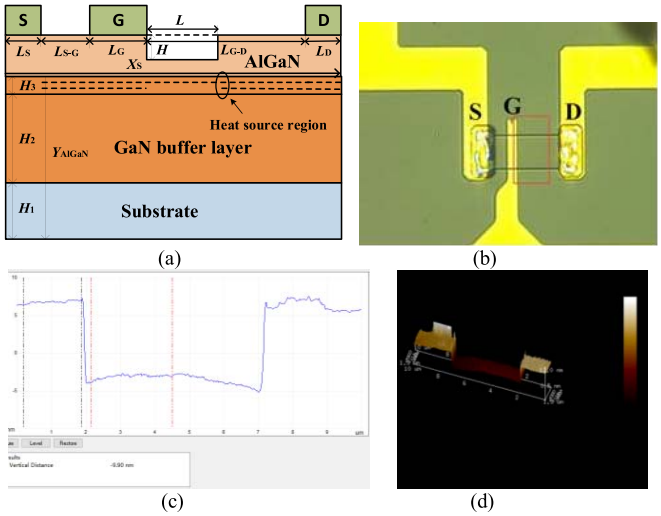

FIGURE 1. **(a) Cross-sectional schematic of AlGaN/GaN HEMT with partial etched AlGaN layer. (b) Microscopic photos of fabricated EAL-HEMT. The AFM 3-D surface morphology (c) and test results (d) of the groove.**

TABLE 1. **The simulation parameeters of the new etched AlGaN/GaN HEMT.**

Symbol	Description	Value
L_S	The length of the source	0.5μm
L_G	The length of the gate	0.5μm
L_D	The length of the drain	0.5μm
$L_{S\text{-}G}$	The distance from the source to the gate	2μm
$L_{G\text{-}D}$	The distance from the gate to the drain	7μm
X_S	The distance from the source	The max=$L_{S\text{-}D}$
L	The length of the groove	--
H	The depth of the groove	--
H_1	The thickness of substrate	50μm
H_2	The thickness of GaN buffer layer	5μm
H_3	The thickness of AlGaN barrier layer	25 nm
Y_{AlGaN}	The distance from the surface of AlGaN barrier layer	--

ICP is used to etch the mesa isolation. The etching depth is 200 nm. The source/drain ohmic contact is Ti/Al/Ni/Au (20 nm/150 nm/50 nm/80 nm). Fig. 1 (c) and (d) show the AFM 3-D surface morphology and test results of the groove. The mesa isolation is annealed for 30 seconds at 850°C in nitrogen atmosphere. The Schottky contact is Ni/Au (20 nm/300 nm). The inner red frame is the position of the etched AlGaN barrier layer. Because the thickness of the groove is only 10 nm, the position cannot be seen clearly under an optical microscope.

An analytical expression is introduced to help understand the temperature distribution inside the device. The governing equation for the heat transfer is Laplace's equation, when the new etched AlGaN/GaN HEMT shown in Fig. 1 (a) is in the on-state.

$$\frac{\partial^2 T_i(x,y)}{\partial x^2} + \frac{\partial^2 T_i(x,y)}{\partial y^2} = 0, \quad i = 1, 2 \tag{1}$$

The boundary conditions for T_i(x,y) in Fig. 2 are:

$$\left.\frac{\partial T_i}{\partial x}\right|_{x=0,L} = 0, \quad \left. k_1 \frac{\partial T_1}{\partial y}\right|_{y=0} = \left. k_2 \frac{\partial T_2}{\partial y}\right|_{y=0} \tag{2}$$

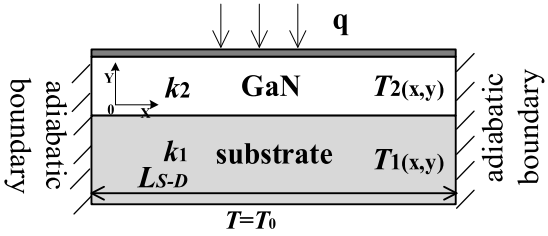

FIGURE 2. The temperature boundaries of new etched AlGaN/GaN HEMT in the on-state.

$$\left.\frac{\partial T_2}{\partial y}\right|_{y=H_2} = -\frac{q}{k},\ P_V = nev_dE \tag{3}$$

$$T_1(x,0) = T_2(x,0), T_1(x,H_1) = T_0 \tag{4}$$

where k_2 and k_1 are the thermal conductivity of the GaN buffer layer and sapphire substrate. P_v is the joule thermal power density, n is the electron concentration, e is the electron charge, v_d is the electron drift velocity and E is the electric field. The solution could be obtained by means of separation of variables. Upon rearranging the above solutions, we obtain the following set of equation.

$$\begin{cases} T_2(x,y) = \sum_{n=1}^{\infty} cos(\lambda_n x)(A_1 sinh(\lambda_n y) + A_2 cosh(\lambda_n y)) \\ \quad +T_0, 0 \le y \le H_2 \\ T_1(x,y) = \sum_{n=1}^{\infty} cos(\lambda_n x)(A_3 sinh(\lambda_n(-H_1 - y)) + T_0, \\ \quad -H_1 \le y \le 0 \end{cases} \tag{5}$$

where the coefficient of A_1, A_2, A_3 and λ_n are shown in Eq. (6-9).

$$\lambda_n = \frac{n\pi}{L_{S-D}} \tag{6}$$

$$A_1 = \frac{-\frac{k_1}{k_2 tanh(\lambda_n H_1 x)} \int_0^L -\frac{q}{k} cos(\lambda_n x)dx}{\frac{L}{2}\lambda_n x\left(-\frac{k_1 cosh(\lambda_n H_2 x)}{k_2 tanh(\lambda_n H_1 x)} + sinh(\lambda_n H_2 x)\right)} \tag{7}$$

$$A_2 = \frac{\int_0^L -\frac{q}{k} cos(\lambda_n x)dx}{\frac{L}{2}\lambda_n x\left(-\frac{k_1 cosh(\lambda_n H_2 x)}{k_2 tanh(\lambda_n H_1 x)} + sinh(\lambda_n H_2 x)\right)} \tag{8}$$

$$A_3 = \frac{\frac{1}{sinh(\lambda_n H_1)} \int_0^L -\frac{q}{k} cos(\lambda_n x)dx}{\frac{L}{2}\lambda_n x\left(-\frac{k_1 cosh(\lambda_n H_2 x)}{k_2 tanh(\lambda_n H_1 x)} + sinh(\lambda_n H_2 x)\right)} \tag{9}$$

There is a strong electric field near the gate of AlGaN/GaN HEMT in on-state. When a large number of carriers pass through this region, its speed continues to accelerate, and energy exchange with the lattice frequently occurs, so a large amount of heat is generated at the interface between AlGaN barrier layer and GaN buffer layer. As shown in Eq. (5), the heat generated by the heterojunction is mainly dissipated by flowing through the sapphire substrate from the GaN layer. The electric field of new etched AlGaN/GaN HEMT is more uniform and lower heat transfer inside the solid medium is beneficial to device performance. The mathematical model provides a theoretical basis for us to analyze the temperature distribution.

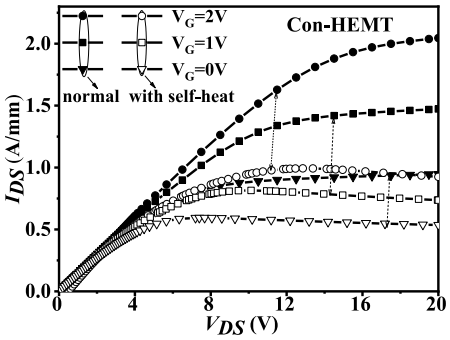

FIGURE 3. Effect of self-heating on output characteristics of AlGaN/GaN HEMT.

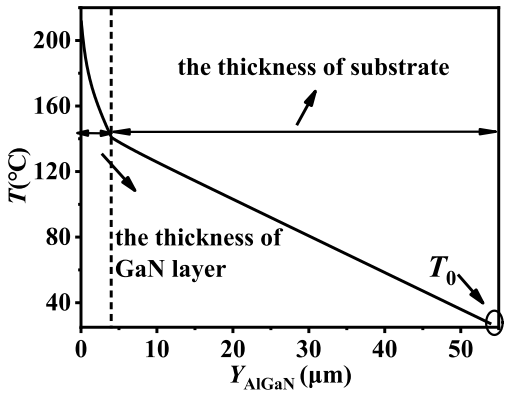

FIGURE 4. Temperature variation trend of AlGaN/GaN HEMT along the substrate direction.

III. PHYSICAL ANALYSIS AND RESULT DISCUSSION

Fig. 3 shows the comparison of output characteristics of conventional AlGaN/GaN HEMT before and after adding thermal field model. Through the simulation results, we can clearly observe the self-heating phenomenon of devices. When the gate bias voltage is the same, the drain output current decreases with the addition of thermal field model. In the saturation region of devices, the leakage saturation current I_{DS} decrease with the increase of drain voltage. Reduction will have a negative impact on the power characteristics and stability of the device.

Fig. 4 is a temperature change trend chart from the device surface to the substrate under the gate. Here the thickness of substrate is set at 50μm. We can see that the temperature of the AlGaN/GaN HEMT decreases rapidly from the barrier layer to the substrate. Because the thickness of the AlGaN barrier layer is relatively thinner than that of the GaN layer, we think that the heat source of the device is distributed in the AlGaN/GaN heterojunction during the temperature analysis. So, we focus on the temperature distribution in the device channel.

Fig. 5 (a) compares the junction temperature distribution of traditional AlGaN/GaN HEMT with EAL-HEMT (H = 5nm and L = 4μm). We can see that the maximum junction temperature of traditional AlGaN/GaN HEMT is 360°C, and the hotspot is located at the gate edge. Under the same bias

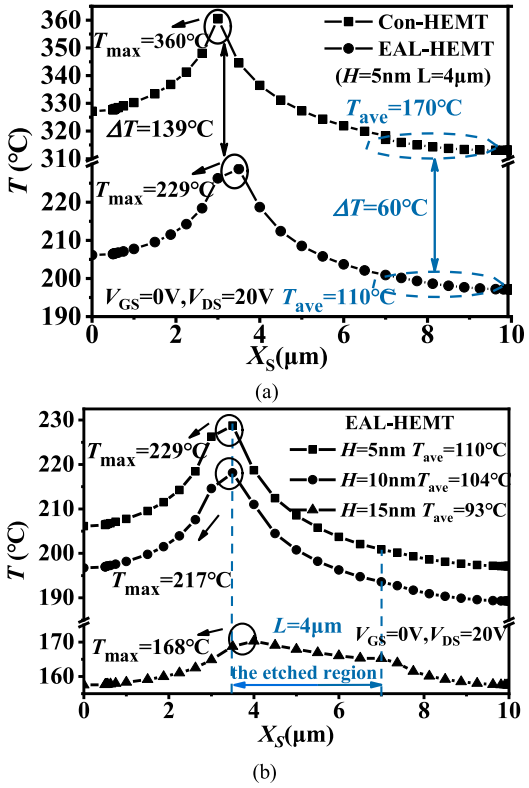

FIGURE 5. (a) The junction temperature distribution of the new etched AlGaN/GaN HEMT (L = 4 μm and H = 5 nm) with traditional AlGaN/GaN HEMT. (b) When L = 4 μm, the junction temperature of AlGaN/GaN HEMT varies with H.

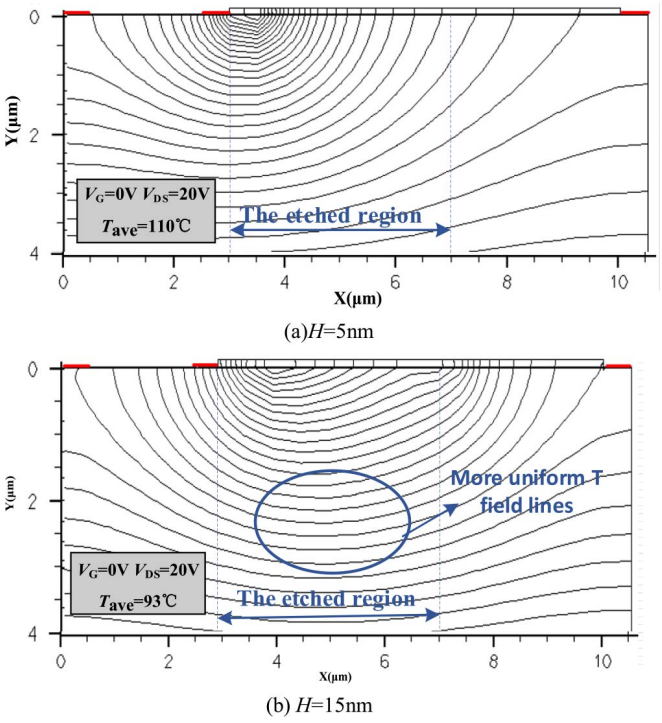

FIGURE 6. When L = 4μm, V_G = 0V and V_{DS} = 20V are constant parameters, isothermal distribution of EAL-HEMT varies with the thickness of groove: (a) H = 5 nm and (b) H = 15 nm.

conditions, the T_{max} and T_{ave} of the etched AlGaN/GaN HEMT are 229°C and 110°C, respectively, which are 36.4% and 35.3% lower than the traditional AlGaN/GaN HEMT, and the hot spot location shift to drain. Due to the zoning change of 2DEG concentration, the strong electric field near the gate in working state decreases, and weak electric field appears in the etched area where the electrons accelerated by the electric field exchange lesser energy with the lattice. Hence, the maximum temperature of the gate edge is transferred to the etching edge. The two high temperature points optimize the temperature distribution at the heterojunction channel, and the average junction temperature is reduced. Fig. 5 (b) shows the variation of junction temperature of L = 4μm EAL-HEMT with H. It can be seen that the junction temperature of the device decreases with the increase of H. When H = 15 nm, the T_{max} and T_{ave} of the AlGaN/GaN HEMT decrease by 53.8% that of traditional structure. It can be seen from the Eq. (5) that A_1, A_2, A_3 are the main factors affecting the temperature, and the strength of the heat source in these is reduced to 0.01% due to the increasing H. The simulation results are consistent with the trend of the formula.

Fig. 6 presents the two-dimensional isotherm distribution of EAL-HEMT, from which we can see the overall temperature distribution trend more intuitively. As shown in Fig. 6 (a), with the etching depth H = 5nm, crowed temperature field lines are formed at the gate edge. The effect of temperature distribution optimization is not obvious, due to small etching thickness. The high temperature at the gate edge is the main reason for the uneven temperature field. When the etching thickness achieves 15nm, the isotherm distribution under the etched AlGaN layer becomes a uniform distribution compared with H = 5nm and the temperature field is symmetrical to the whole HEMT. With the increase of etching depth H, the isotherm distribution in the device becomes more uniform, and the slope of the isotherm at the same location of the device becomes smaller. The situation shown in Fig. 6 (b) is more advantageous for us when we focus on the high temperature characteristics of the device.

Fig. 7 shows the variation of junction temperature distribution of the new etched AlGaN/GaN HEMT with L when V_{GS} = 0V, V_{DS} = 20V and H = 15nm. The simulation results show that when L is 2μm, 3μm, 4μm and 5μm, T_{max} is 177°C, 171°C, 168°C and 159°C respectively. We can see that with the increase of L, the peak temperature near the gate decreases, and a new hot spot appear in the channel. However, there is little difference in average junction temperature with the increasing L, which indicates that the influence of etched AlGaN thickness on the junction temperature distribution is greater than that of length. With the increasing etching depth, the 2DEG induced by polarization effect gradually decreases under the etched region. Since the heat is generated from the electric field to work on the electrons, the channel below the etched layer generates

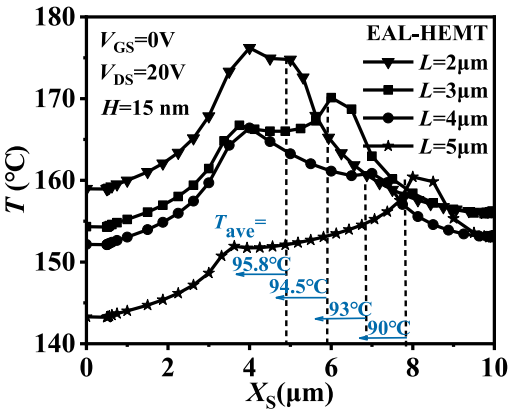

FIGURE 7. Channel temperature of the new etched AlGaN/GaN HEMT with different length.

less heat and has a lower junction temperature than the other parts. Therefore, the increase in etching depth and length is an effective method to reduce the junction temperature, but the effect of the etching depth is more significant.

IV. MEASUREMENT OF JUNCTION TEMPERATURE BY RAMAN SPECTROSCOPY

The instrument used in the experiment is Labram HR 800 laser confocal Raman spectrometer. The light source is an Ar + laser source with 532 nm wavelength. The energy of the light source is 2.45 eV. The direction of the incident light is parallel to the polar C axis of the material, and the illumination area is about 1μm^2. The optical microscopic objective used in the experiment has a magnification of 100 times, a numerical aperture of 0.9 and an optical resolution of 0.61 λ/NA. Fig. 8 (a) shows the typical Raman spectra of GaN material at room temperature in non-working state. To detect the scattering spectra of the material more effectively, this experiment observes the E_2 mode phonon with strong Raman frequency shift. Then, the junction temperature is measured.

We need to calibrate the phonon frequency shift before the measurement to get the actual channel temperature, because the scattering frequency of the phonon is a function of temperature and conforms to Cui's theorem [13]. The phonons frequency shifts changes approximately linearly with temperature and the temperature dependence coefficient T_{de} equals to -0.01259 cm^{-1}. By the temperature dependence coefficient, we can translate the phonons frequency shift into the junction temperature distribution.

Fig. 8 (b-d) display results of the junction temperature distribution with 0.3μm lateral steps at different power dissipations. Different power dissipation (P_{diss}) is obtained by increasing drain voltage under the condition of zero gate bias voltage. It shows that for the same AlGaN/GaN HEMT, the overall temperature distribution increases with the power dissipation. The reason for this phenomenon is obvious. The increased power dissipation means that the more power is lost due to heat emission. Therefore, the average temperature

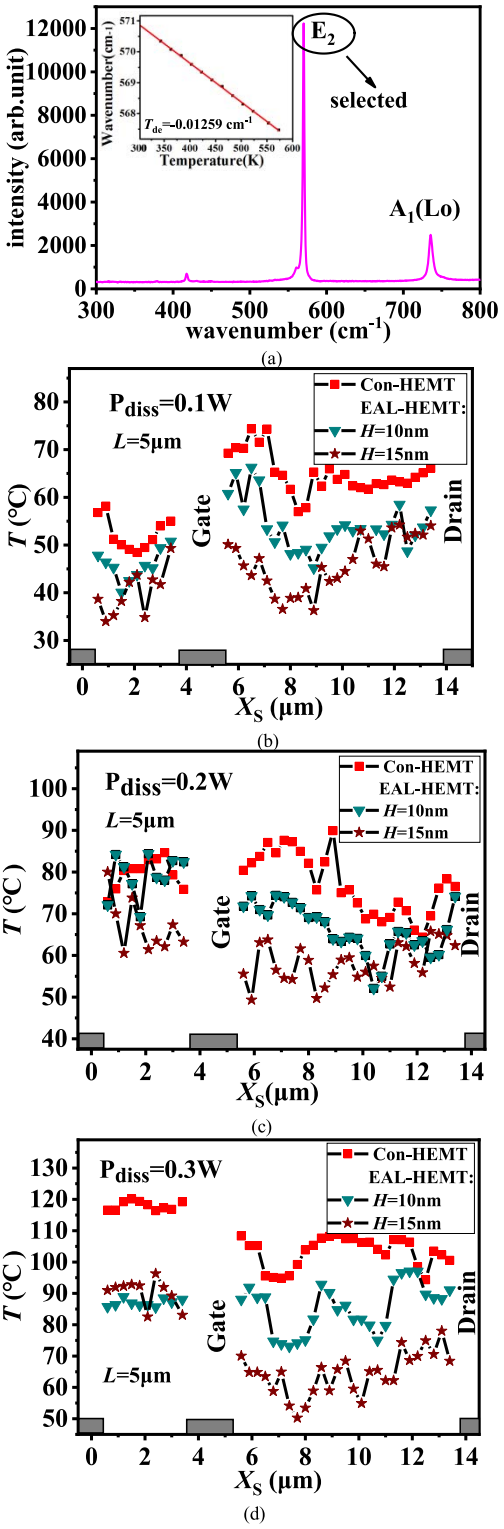

FIGURE 8. (a) Typical GaN Raman spectra and the temperature dependence coefficient $T_{de} = -0.01259$ cm^{-1}. Temperature map of AlGaN/GaN HEMT with partial etched AlGaN layer on sapphire at (a) P_{diss} = 0.1W, (b) P_{diss} = 0.2W, and (c) P_{diss} = 0.3W. Temperature line scans from the source to the drain with 0.3μm lateral step size.

of the device will be rise. In addition, we can also observe that the channel junction temperature of the EAL- HEMT is lower than that of the ordinary AlGaN/GaN HEMT under

TABLE 2. The average junction temperature of AlGaN/GaN HEMTs.

P_{diss}(W)	Con-HEMT T_{ave}(℃)	H=5 nm T_{ave}(℃)	H=10m T_{ave}(℃)	H=15nm T_{ave}(℃)
0.1	61.7	56.8	51.9	44.2
0.2	77.8	69.3	60.0	51.5
0.3	103.4	93.4	85.3	72.1

the same conditions, and the junction temperature decreases with the increasing etched thickness, which is consistent with the conclusion obtained by ISE TCAD simulation mentioned in the previous chapter.

Table 2 is the average junction temperature statistics of AlGaN/GaN HEMTs. When the power dissipation is 0.3 W and the etched thickness is 15 nm, the average junction temperature of the new etched AlGaN/GaN HEMT is 30.3% lower than that of the ordinary AlGaN/GaN HEMT, and the new etched AlGaN/GaN HEMT with $H = 5$ nm is 22.8% lower. Similarly, when the power dissipation is 0.2 W and 0.1 W, the T_{ave} of the $H = 15$ nm new etched AlGaN/GaN HEMT compared with that of the ordinary structure and the $H = 5$ nm new etched AlGaN/GaN HEMT, are reduced by 33.8%, 25.7% and 28.4%, 22.2% respectively. By measuring, we can see that the channel temperature of AlGaN/GaN HEMTs can be effectively reduced by etching the AlGaN barrier layer.

V. CONCLUSION

In conclusion, we have discussed the thermal field of the new AlGaN/GaN HEMT with partial etched AlGaN. On the basis of the mathematical model, novel AlGaN/GaN HEMT is helpful to optimize the temperature distribution and reduce junction temperature. The simulation results of the junction temperature distribution and isothermal distribution indicate that the new etched AlGaN/GaN HEMT is super than conventional AlGaN/GaN HEMT. Then the junction temperature of fabricated new etched AlGaN/GaN HEMT is measured by Raman spectroscopy. This method has a spectral resolution of 1μm and a temperature accuracy of 10°C. We can get the result that when the power dissipation is 0.3W, the average junction temperature of the new etched AlGaN/GaN HEMT with 15 nm etched thickness reduced by 30.3%. Both the simulation results and measurement results confirm what we have been put forward: new AlGaN/GaN HEMT with partial etched AlGaN layer has a great significance for reducing the self-heating effect and improving the high temperature stability.

REFERENCES

[1] P. M. Asbeck, E. T. Yu, S. S. Lau, G. J. Sullivan, J. Van Hove, and J. Redwing, "Piezoelectric charge densities in AlGaN/GaN HFETs," *Electron. Lett.*, vol. 33, no. 4, pp. 1230–1231, Jul. 1997, doi: 10.1049/el:19970843.

[2] O. Ambacher *et al.*, "Two dimensional electron gases induced by spontaneous and piezoelectric polarization in undoped and doped AlGaN/GaN heterostructures," *J. Appl. Phys.*, vol. 87, no. 1, pp. 334–344, 2000, doi: 10.1063/1.369664.

[3] M. Miyoshi, T. Egawa, and H. Ishikawa, "Structural characterization of strained AlGaN layers in different Al content AlGaN/GaN heterostructures and its effect on two-dimensional electron transport properties," *J. Vac. Sci. Technol. B Microelectron. Nanometer Struct. Process. Meas. Phenom.*, vol. 23, no. 4, pp. 1527–1531, 2005, doi: 10.1116/1.1993619.

[4] R. Gaska, A. Osinsky, J. W. Yang, and M. S. Shur, "Self-heating in high-power AlGaN-GaN HFETs," *IEEE Electron Device Lett.*, vol. 19, no. 3, pp. 89–91, Mar. 1998, doi: 10.1109/55.661174.

[5] A. Aouf, F. Djeffal, and F. Douak, "Thermal stability investigation of power GaN HEMT including self-heating effects," in *Proc. 6th Int. Conf. Syst. Control (ICSC)*, Batna, Algeria, 2017, pp. 451–454, doi: 10.1109/ICoSC.2017.7958745.

[6] E. R. Heller and A. Crespo, "Electro-thermal modeling of multifinger AlGaN/GaN HEMT device operation including thermal substrate effects," *Microelectron. Rel.*, vol. 48, no. 1, pp. 45–50, 2008, doi: 10.1016/j.microrel.2007.01.090.

[7] Y. R. Wu and J. Singh, "Transient study of self-heating effects in AlGaN/GaN HFETs: Consequence of carrier velocities, temperature, and device performance," *J. Appl. Phys.*, vol. 101, no. 11, 2007, Art. no. 113712, doi: 10.1063/1.2745286.

[8] F. Bertoluzza, N. Delmonte, and R. Menozzi, "Three-dimensional finite-element thermal simulation of GaN-based HEMTs," *Microelectron. Rel.*, vol. 49, no. 5, pp. 468–473, 2009, doi: 10.1016/j.microrel.2009.02.009.

[9] N. Killat, M. Kuball, T.-M. Chou, U. Chowdhury, and J. Jimenez "Temperature assessment of AlGaN/GaN HEMTs: A comparative study by Raman, electrical and IR thermography," in *Proc. IEEE Int. Rel. Phys. Symp.*, Anaheim, CA, USA, 2010, pp. 528–531, doi: 10.1109/IRPS.2010.5488777.

[10] V. Sodan *et al.*, "Experimental benchmarking of electrical methods and μ-Raman spectroscopy for channel temperature detection in AlGaN/GaN HEMTs," *IEEE Trans. Electron Devices*, vol. 63, no. 6, pp. 2321–2327, Jun. 2016, doi: 10.1109/TED.2016.2550203.

[11] R. Yamaguchi, Y. Suzuki, J. T. Asubar, H. Tokuda, and M. Kuzuhara, "Reduced current collapse in multi-fingered AlGaN/GaN MOS-HEMTs with dual field plate," in *Proc. IEEE Int. Meeting Future Electron Devices Kansai (IMFEDK)*. Kyoto, Japan, 2017, pp. 92–93, doi: 10.1109/IMFEDK.2017.7998058.

[12] Y. Song, B. Duan, X. Yuan, Z. Cao, H. Guo, and Y. Yang, "New Al 0.25 Ga 0.75 N/GaN high electron mobility transistor with partial etched AlGaN layer," *Superlattices Microstruct.*, vol. 93, pp. 303–307, 2016, doi: 10.1016/j.spmi.2016.03.039.

[13] J. B. Cui, K. Amtmann, J. Ristein, and L. Ley, "Noncontact temperature measurements of diamond by Raman scattering spectroscopy," *J. Appl. Phys.*, vol. 83, no. 12, pp. 7929–7933, 1998, doi: 10.1063/1.367972.